THE MULTIPLE VORTEX NATURE OF TROPICAL CYCLOGENESIS

A Thesis

by

JASON ALLEN SIPPEL

Submitted to the Office of Graduate Studies of
Texas A&M University
in partial fulfillment of the requirements for the degree of

MASTER OF SCIENCE

December 2004

Major Subject: Atmospheric Sciences

THE MULTIPLE VORTEX NATURE OF TROPICAL CYCLOGENESIS

A Thesis

by

JASON ALLEN SIPPEL

Submitted to the Office of Graduate Studies of
Texas A&M University
in partial fulfillment of the requirements for the degree of

MASTER OF SCIENCE

Approved as to style and content by:

Richard Orville
(Head of Department)

John Nielsen-Gammon
(Chair of Committee)

Craig Epifanio
(Member)

Fuqing Zhang
(Member)

Hongxing Liu
(Member)

December 2004

Major Subject: Atmospheric Sciences

ABSTRACT

The Multiple Vortex Nature of Tropical Cyclogenesis. (December 2004)

Jason Allen Sippel, B.S., Texas A&M University

Chair of Advisory Committee: Dr. John Nielsen-Gammon

This thesis contains an observational analysis of the genesis of Tropical Storm Allison (2001). Using a paradigm of tropical cyclone formation as the superposition of potential vorticity (PV) anomalies, the importance of different scales of PV merger to various aspects of Allison's formation is discussed. While only the case of Allison is discussed in great detail, other studies have also documented PV superposition on various scales, and superposition *could* be important for most tropical cyclones.

Preceding Allison's genesis, PV superposition on the large scale destabilized the atmosphere and increased low-level cyclonic vorticity. This presented a more favorable environment for the formation of MCV-type PV anomalies and smaller, surface-based, meso-β-scale vortices. Although these vortices eventually merged to form a more concentrated vortex with stronger surface pressure gradients, the merger happened well after landfall of Allison and no strengthening ensued.

The unstable, vorticity-rich environment was also favorable for the development of even smaller, meso-γ-scale vortices that accompanied deep convective cells within one of Allison's meso-β-scale vortices. The observations herein suggest that the meso-γ-scale convective cells and vortices are the respective source of PV production and building blocks for the meso-β-scale vortices.

Finally, this thesis discusses issues related to the multiple vortex nature of tropical cyclone formation. For instance, the tracking of developing tropical cyclones is greatly complicated by the presence of multiple vortices. For these cases, the paradigm of a single cyclone center is inappropriate and alternative tracking methods are introduced.

ACKNOWLEDGEMENTS

The author would like to thank John Nielsen-Gammon of Texas A&M University and Steve Allen of the Houston/Galveston National Weather Service Forecast Office.

TABLE OF CONTENTS

LIST OF FIGURES

FIGURE Page

LIST OF TABLES

1. INTRODUCTION

Forecasts of the timing and details of tropical cyclone formation have fallen far behind those of tropical cyclone intensity and position during the past 50 years. Track forecasts have improved considerably during this period, and while intensity forecast skill has lagged somewhat (DeMaria and Gross 2003), cyclogenesis forecasts have proven to be more difficult. Although the scientific and operational communities now understand which environments are favorable for tropical cyclone formation, they are still unable to accurately forecast the evolution from a tropical disturbance to a tropical cyclone (Emanuel, 2003). The most obvious reason for this is has been the lack of understanding of tropical cyclogenesis. Air-sea instability theory (Emanuel 1986; Rotunno and Emanuel 1987) has been accepted as the leading theory for cyclone maintenance and intensification (Craig and Gray 1996), but it relies on the presence of an initial finite-amplitude vortex (Rotunno and Emanuel 1987; Emanuel 1989) and gives no indication how such a vortex arises from a tropical disturbance.

Recent observational and numerical studies have shed light on the initial stages of tropical cyclogenesis in a variety of environments, suggesting that vortex merger on a variety of scales plays an important role in the cyclogenesis process. From the potential vorticity (PV) point of view (Hoskins et al. 1985), the horizontal or vertical superposition of PV anomalies of the same sign will strengthen, deepen, and widen the circulation associated with both anomalies. If the resulting circulation is able to reach the surface with sufficient intensity, then the initial disturbance requirement of air-sea

---

This thesis follows the style of *Monthly Weather Review*.

interaction can be met. Furthermore, cumulus convection tends to redistribute PV downwards (Raymond and Jiang, 1990), and surface-based convection can thereby enhance surface vortex formation. If sustained convection develops within a large reservoir of mid- or upper-level PV, there is enhanced potential to create a low-level disturbance of sufficient amplitude for air-sea interaction to commence.

Both horizontal and vertical PV superposition seem to be at work in the monsoon environment of the west Pacific where much of the observational work into the early stages of tropical cyclogenesis has been concentrated. Simpson et al. (1997) discuss a case where two tropical mesoscale convective systems (MCSs) and their embedded PV anomalies (mesoscale convective vortices, or MCVs) merge, resulting in a tropical cyclone. Meanwhile, during the formation of Typhoon Irving (1992) in the West Pacific (Ritchie and Holland 1997) the interactions between multiple MCVs and a tropical upper-tropospheric trough (TUTT) led to tropical cyclogenesis over a period of about a week. A tropical depression emerged only after convection associated with the TUTT redistributed its PV to the surface and enhanced the circulation of the merged MCVs.

Multi-scale vortex superposition also played an important role in the development of Typhoon Robyn (1993). In this case, Harr et al. (1996) document the formation and decay of several MCSs within a larger-scale monsoon depression. As one MCS developed within the depression, its associated PV anomaly superposed onto the larger-scale PV anomaly and the larger-scale circulation center shifted towards the position of the MCS. This MCS decayed but was followed another MCS that formed near the 700 hPa circulation center. The authors hypothesized that the formation of this

second MCS eventually contributed to the formation of the tropical depression. In this scenario, superposition of PV from the two MCSs onto the larger-scale PV structure helped create a surface vortex of tropical depression strength.

Vortex merger on the mesoscale is important for at least some cases of tropical cyclogenesis in the Atlantic and Pacific. For example, Hendricks et al. (2004) used a 3 km MM5 simulation to infer a two-phase evolution during the genesis of Hurricane Diana (1984). During the first phase, intense convective bursts generate multiple small-scale PV anomalies, and during the second stage multiple mergers of these vortices lead to larger-scale momentum spin-up. Supporting the idea that small-scale vortices can merge and act as PV building blocks for tropical cyclones is an observational analysis of the formation of Tropical Cyclone Ed (1993) near Guam (Stewart and Lyons 1996). The cyclone's nascent eyewall absorbed a series of convective scale vortices that were strong enough to trip the mesocyclone algorithm of the Guam WSR-88D. Their absorption into the eyewall directly preceded the rapid intensification of the cyclone. Multiple mesoscale vortices are also frequently noted by the Tropical Prediction Center (TPC). Published cases of such vortices in the Atlantic include Isabel (1958) (Stossmeister and Barnes 1992) and Gustav (2002) (Hendricks et al. 2004).

Although convective- and larger-scale superposition has not previously been documented to occur simultaneously, there appears to be no reason why this should not occur. For example, the disturbance that preceded Hurricane Diana (1984) originally deepened as a moist baroclinic cyclone when an upper-level PV anomaly approached a stalled surface front (Davis and Bosart 2001). In this case, the modest baroclinic

strengthening had an effect similar to large-scale PV superposition by strengthening the low-level vorticity. It also helped to focus convection along the front near the low-level vortex. These factors were crucial for the rapid development of stronger surface PV anomaly. With ample deep convection, the enhanced low-level vorticity primed the environment for the small-scale PV anomalies that merged to build the cyclone in the Hendricks et al. (2004) simulation.

The goal of this study is to consider tropical cyclogenesis and intensification as a multiscale superposition of PV anomalies. Although synoptic scale superposition does not directly lead to a tropical cyclone scale vortex, it can enhance low-level vorticity and destabilize the atmosphere by cooling the middle and upper troposphere while enhancing surface fluxes. Such large scale superposition is not essential; in other instances a single PV anomaly or tropical wave can instigate sufficient deep convection such that PV redistribution enhances low-level vorticity and surface fluxes. The MCV-type PV anomalies that form with episodes of deep convection might also merge and produce similar low-level effects.

In any case, the enhanced vorticity and decreased stability which favor tropical cyclogenesis in a climatological sense (Gray 1968; McBride and Zehr 1981) serve as an atmospheric primer for the convective development of small mesoscale PV features. These features can then merge and act as the actual building blocks of tropical cyclones. This type of merger can be an important strengthening and organization mechanism even when the winds are well above tropical storm strength (e.g., strengths at which air-sea interaction instability is thought to be the main contributor to storm intensification).

While the details of each individual event will differ, this seems to be the pattern that many cases follow.

In the current study, this paradigm will be used to investigate the genesis of Tropical Storm Allison (2001). Allison made landfall along the upper Texas coast in June 2001 and is typical of many Gulf of Mexico tropical cyclogenesis events. The storm is an excellent candidate for such a study because its formation occurred completely within range of the KHGX (Houston/Galveston National Weather Service Office) WSR-88D and because the storm made landfall in a dense surface observation network.

Information about synoptic background associated with Allison and a general description of the storm itself can be found in Section 2 of this paper. In Section 3, detail is given on the evolution of the storm along with observational evidence for multiple vortices and vortex merger. Section 4 contains a discussion of various issues related to mesoscale vortices. In addition to concluding remarks, Section 5 gives attention to the applicability of this new paradigm to the operational community. Its use can greatly facilitate the tracking of developing tropical cyclones; alternative tracking methods and their caveats will be presented.

2. BACKGROUND

The thermodynamic environment that preceded Allison's development was typical of that associated with a weak upper level positive PV disturbance in that location and time of year. Substantial convective instability marked the synoptic scale as the return flow on the west side of an East Coast anticyclone pushed a tropical airmass into South Texas, significantly deepening the moist layer. Fig. 1 shows the weak upper level-trough that moved over the Texas coast and the northwest Gulf of Mexico during this time. The weak but sustained large-scale ascent ahead of this trough helped destabilize the atmosphere along the Texas coast, as evidenced by soundings from Brownsville and Corpus Christi on 4 and 5 June. At 0000 UTC 4 June, Brownsville's sounding (Fig. 2a) indicates moderate levels of convective inhibition (CIN) and high levels of convective available potential energy (CAPE) with the moist layer extending to roughly 900 hPa. By 0000 UTC 5 June (Fig. 2b) the CAPE had increased slightly, CIN had disappeared, and the moist layer had deepened to 750 hPa.

Although the thermodynamic environment was favorable for convection over the western Gulf of Mexico, the shear in this region made it initially unfavorable for tropical development. Scatterometer-derived surface winds exceeded 10 m s^{-1} over much of the western Gulf of Mexico on 4 June, and this southeasterly flow strengthened with height to a 20 m s^{-1} 850 hPa low level jet. The low-level flow was somewhat weaker nearer the Texas coast. With the presence of an upper-level trough, the southwesterlies at 300 hPa had strengthened to 10 m s^{-1} over the western Gulf and to over 20 m s^{-1} along the

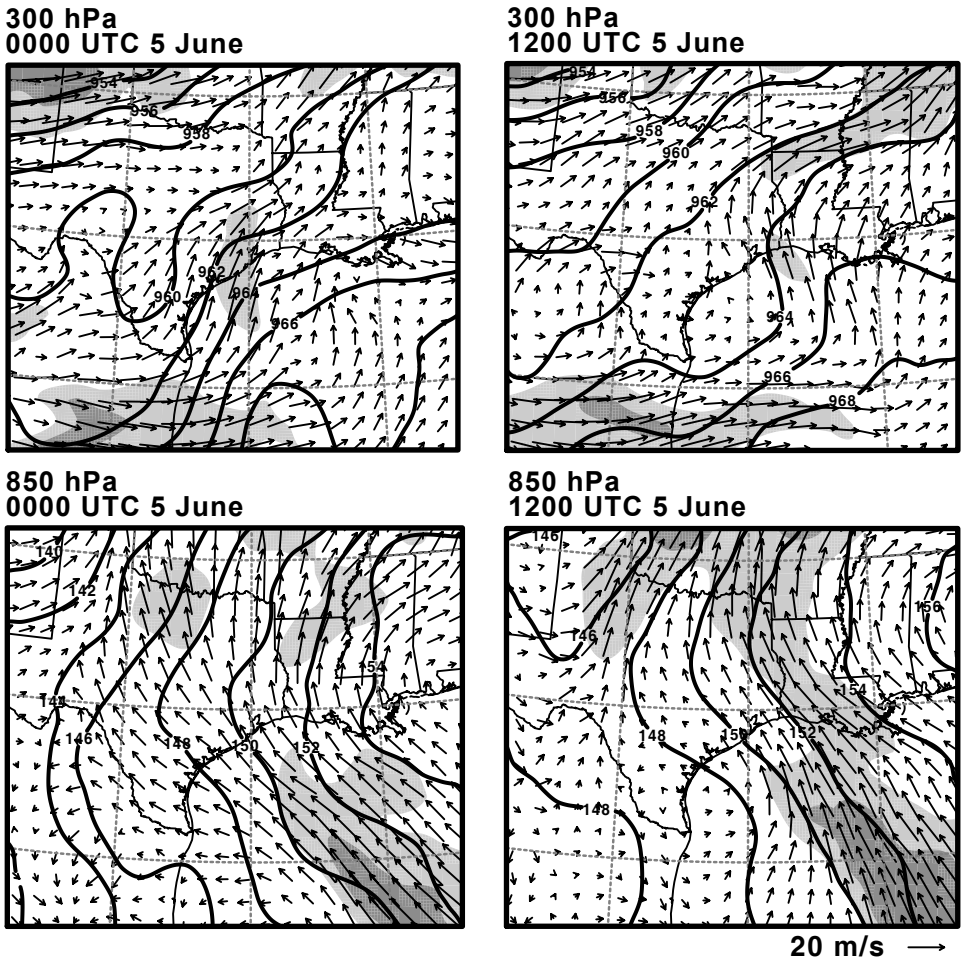

FIG. 1: ETA analyses of 300 hPa and 850 hPa heights and winds for 0000 UTC and 1200 UTC 5 June. Light gray shading is for wind speeds in excess of 15 m s^{-1}, and darker gray represents wind speeds greater than 20 m s^{-1}.

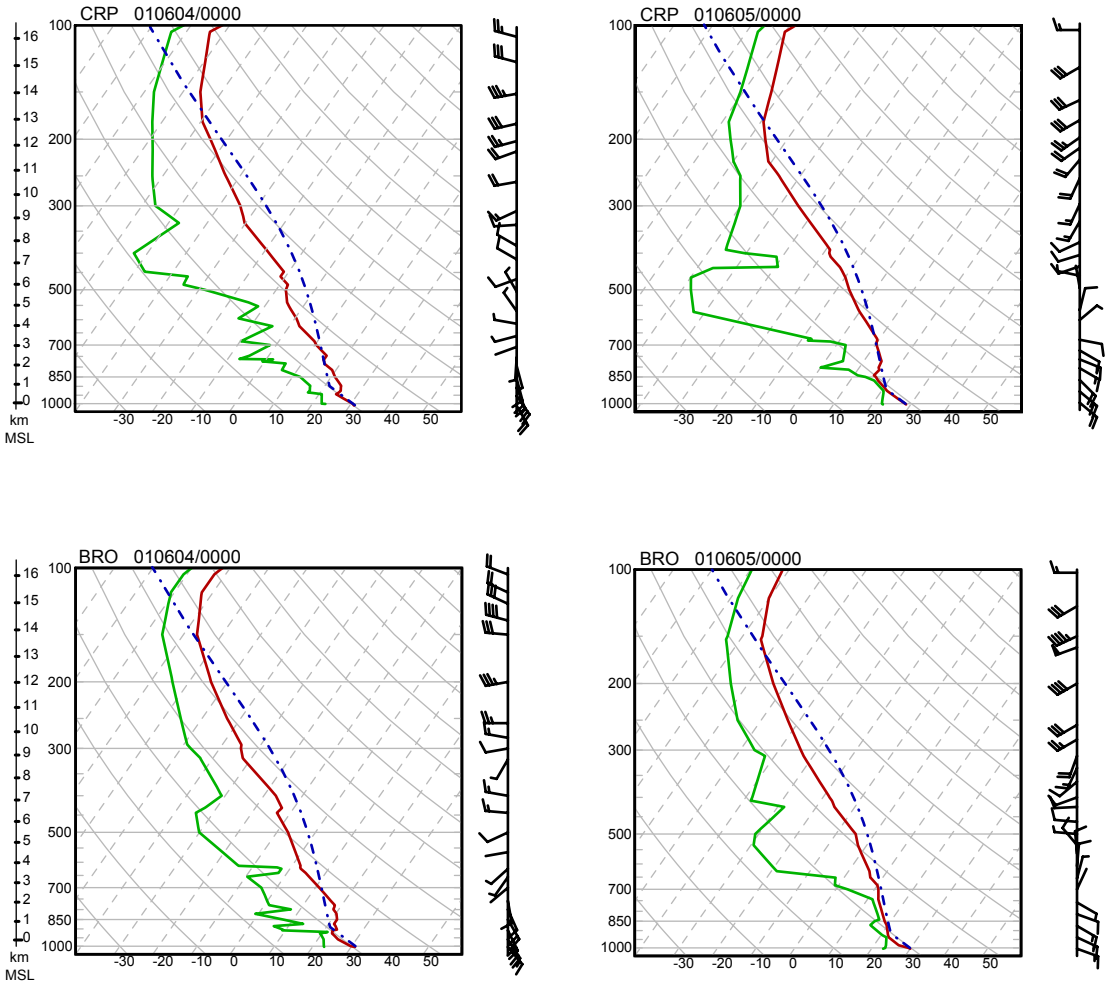

FIG. 2: Soundings from Corpus Christi (CRP) and Brownsville (BRO) from 0000 UTC 4 and 5 June. Dew point is shaded in solid green, temperature in red, and the lifted surface-based parcel trajectory in blue dash-dot.

Texas coast. This implies zonal wind shear over the entire western Gulf of about 20 m s^{-1} , which is unfavorable for tropical development (DeMaria et al. 2001). However, by 1200 UTC 5 June the upper level trough had become reoriented such that weak winds in its axis and southeasterly winds downstream of it were directly over the area of strong surface winds. This is important because the surface winds likely played a critical role in developing a moist boundary layer and destabilizing the atmosphere by inducing intense oceanic surface fluxes. Thus, the shear substantially decreased over an area of high surface fluxes, which is where Allison formed.

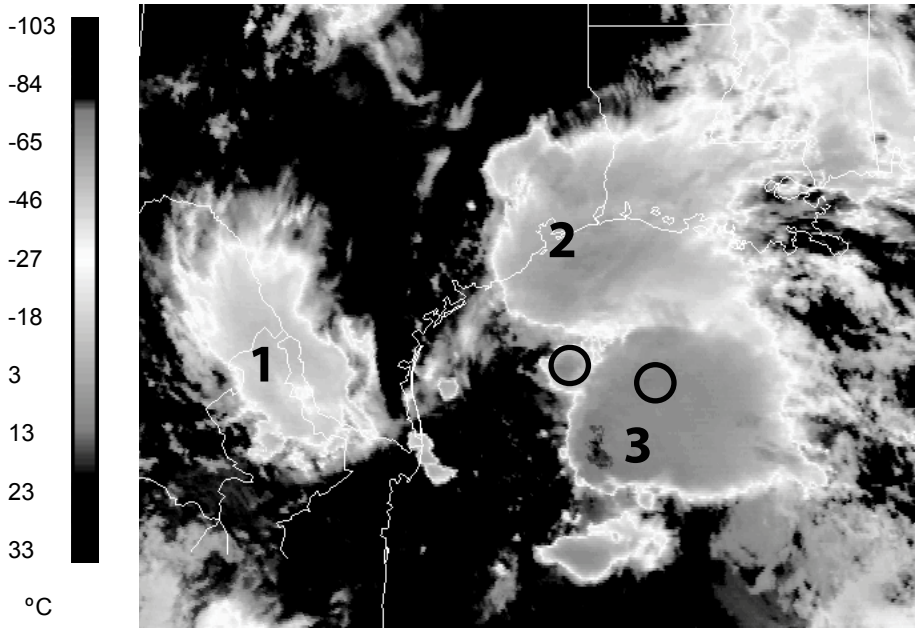

FIG. 3: GOES 8 IR image of Allison's initial convective burst and ongoing MCSs at 0845 UTC 5 June. Each number represents a distinct MCS, and the two bold circles denote the two convective areas in which vortices A and B developed.

Allison quickly developed amidst a series of MCSs that formed along a north-south line near the 500 hPa trough axis on the evening of 4 June. The first convective burst associated with the primary circulation center (westernmost circle in Fig. 3) began around 0800 UTC. Reflectivity data from KHGX clearly indicated that a mesoscale vortex existed through the convective steering levels before reconnaissance aircraft arrived near 1900 UTC. With flight-level observations, the aircraft confirmed the system as a tropical storm and estimated 25 m s^{-1} surface winds and a 1004 hPa surface low. Although the estimated strength remained nearly constant until landfall of the system, the highest sustained surface winds measured along the coast were only about 15 – 20 m s^{-1}.

Allison's surface wind distribution was highly asymmetric, and strong winds were not confined to the circulation center. The surface anticyclone to the east of Allison resulted in a substantial pressure gradient over the central Gulf of Mexico. Multiple oil platforms and ships reported tropical storm force winds hundreds of kilometers from the center of circulation. As Allison made landfall, a ship south of Mobile, AL reported winds in excess of tropical storm force. Meanwhile, surface wind speeds on the west side of the circulation were generally less than 10 m s^{-1}.

A broad, low-level circulation and multiple circulation centers made tracking the system difficult. According to TPC advisories issued in real time, Allison did not make landfall until after 0400 UTC on 6 June near Galveston. The best-track post-analysis issued by the same agency shows the storm making landfall before 0000 UTC. In consideration of such tracking problems, alternatives to the current tracking method for

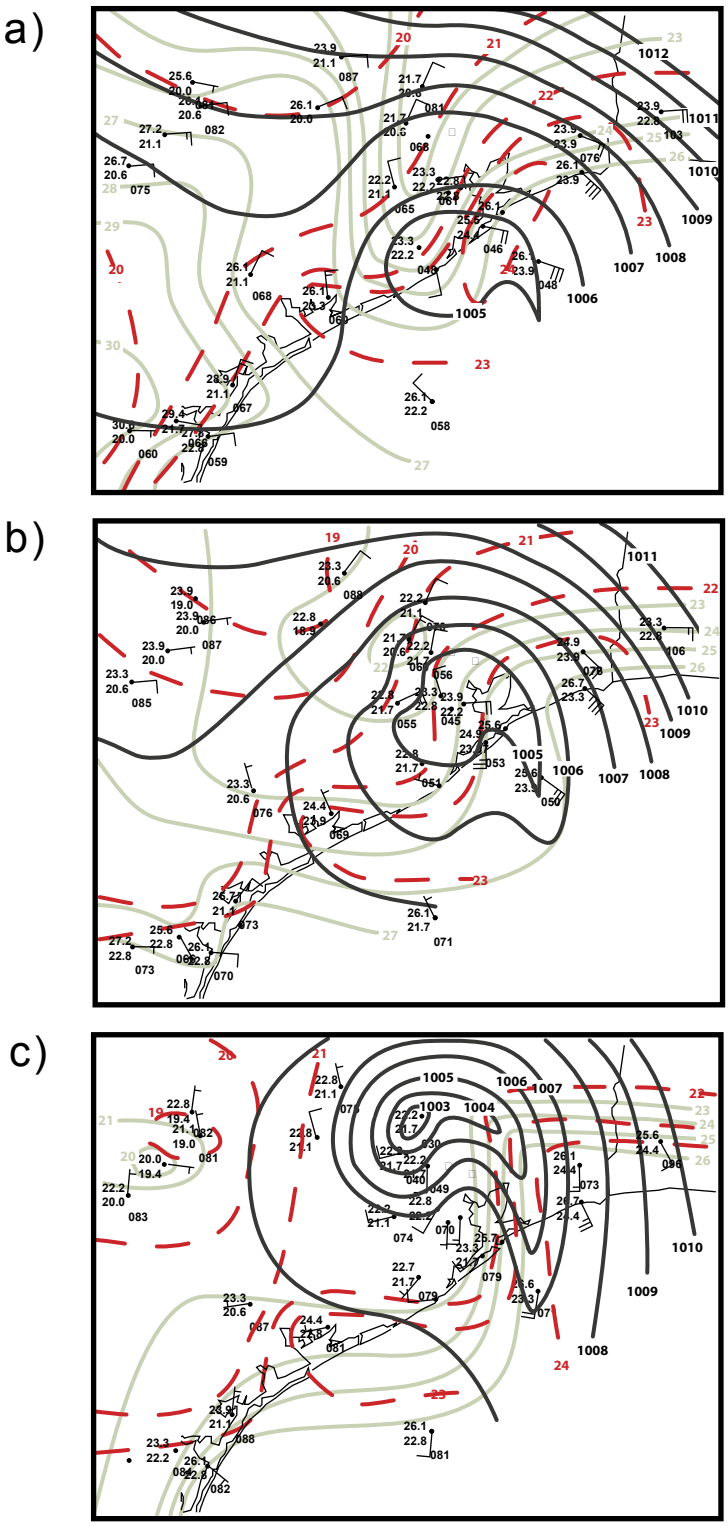

FIG 4: Mesoscale surface analyses for a) 0000 UTC, b) 0200 UTC, and c) 0600 UTC on 6 June. Wind barbs are in m s^{-1} and analyzed fields are as follows: pressure (thick black lines) contoured every 1 hPa, temperature (thick green lines), and dew point (thick red dashed lines) contoured every 1ºC.

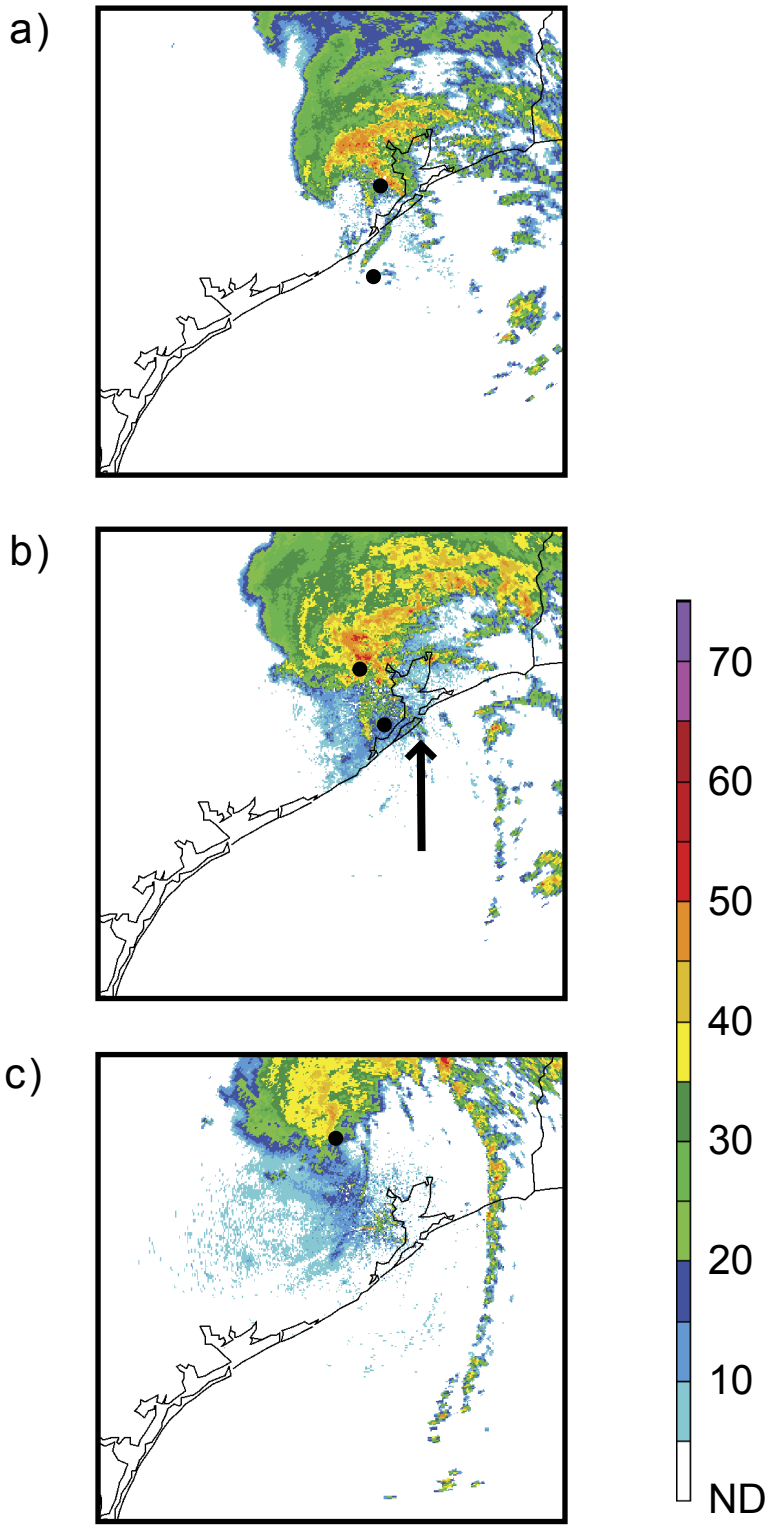

FIG. 5: League City Doppler radar images from a) 0000 UTC, b) 0200 UTC, and c) 0600 UTC 6 June. Arrow in b denotes minor banding around vortex B. Black dots denote center(s). NIDS format radar data is utilized for this study. Scale on right is in dBZ.

developing tropical cyclones will be discussed later in this study.

Mesoscale analyses of Allison during her landfall reveal the development an interesting frontal structure with the system in the absence of any synoptic-scale baroclinic zone. During the hours before the storm made landfall, a substantial cold pool associated with precipitation that preceded Allison's landfall formed just inland over Southeast Texas. The mesoscale analyses shown in Fig. 4 show the development of surface fronts with cross-frontal temperature differences of about 4ºC as the circulation began to interact with the cold pool. The structure quickly evolved into something reminiscent of an occluded mid-latitude cyclone, with the surface low connected to the frontal features by only a pressure trough.

Fig. 5 shows the response of the precipitation distribution to this structure. All convective precipitation near the center gradually vanished as a rainband just east of the leading edge of the cold pool became the focus for convection. Meanwhile, a large area of stratiform precipitation formed north of the effective warm front. The limited amount of surface data available over eastern Texas indicates that the frontal structure remained through at least 1200 UTC 6 June.

3. SYSTEM EVOLUTION

a. Synoptic and meso-α scales

Allison evidently formed in conjunction with PV superposition on multiple scales. On the synoptic scale, the analyses from multiple operational models indicated a low-level PV anomaly associated with the low-level jet that was distinctly different from the anomaly at mid and upper levels. This feature, shown in the ETA analyses in Fig. 6, moved into the Gulf of Mexico from the southeast. Meanwhile the upper-level trough, also shown in Fig. 6, approached from over Mexico and superposed onto the lower anomaly. While convection did exist with the low-level disturbance during the previous days, its area was limited and Allison did not form until the features at both levels superposed.

The pre-Allison environment was quite supportive of developing mesoscale PV anomalies, thereby enhancing the probability of superposition and cyclogenesis. Infrared satellite loops indicated a low- to mid- level mesoscale (~250 km) circulation directly over the area where one of Allison's initial convective bursts developed shortly before 0900 UTC 5 June. Extrapolating the track of this circulation backward in time reveals that it may have developed hours earlier under the anvil region of a previous MCS. Although this feature was unresolved by numerical models, its history and scale imply that it was likely an MCV-type PV feature. As further evidence of this environment's ability to produce MCVs, another such PV anomaly developed on the morning of 5 June over the Rio Grande Valley of northeast Mexico (see Fig. 7).

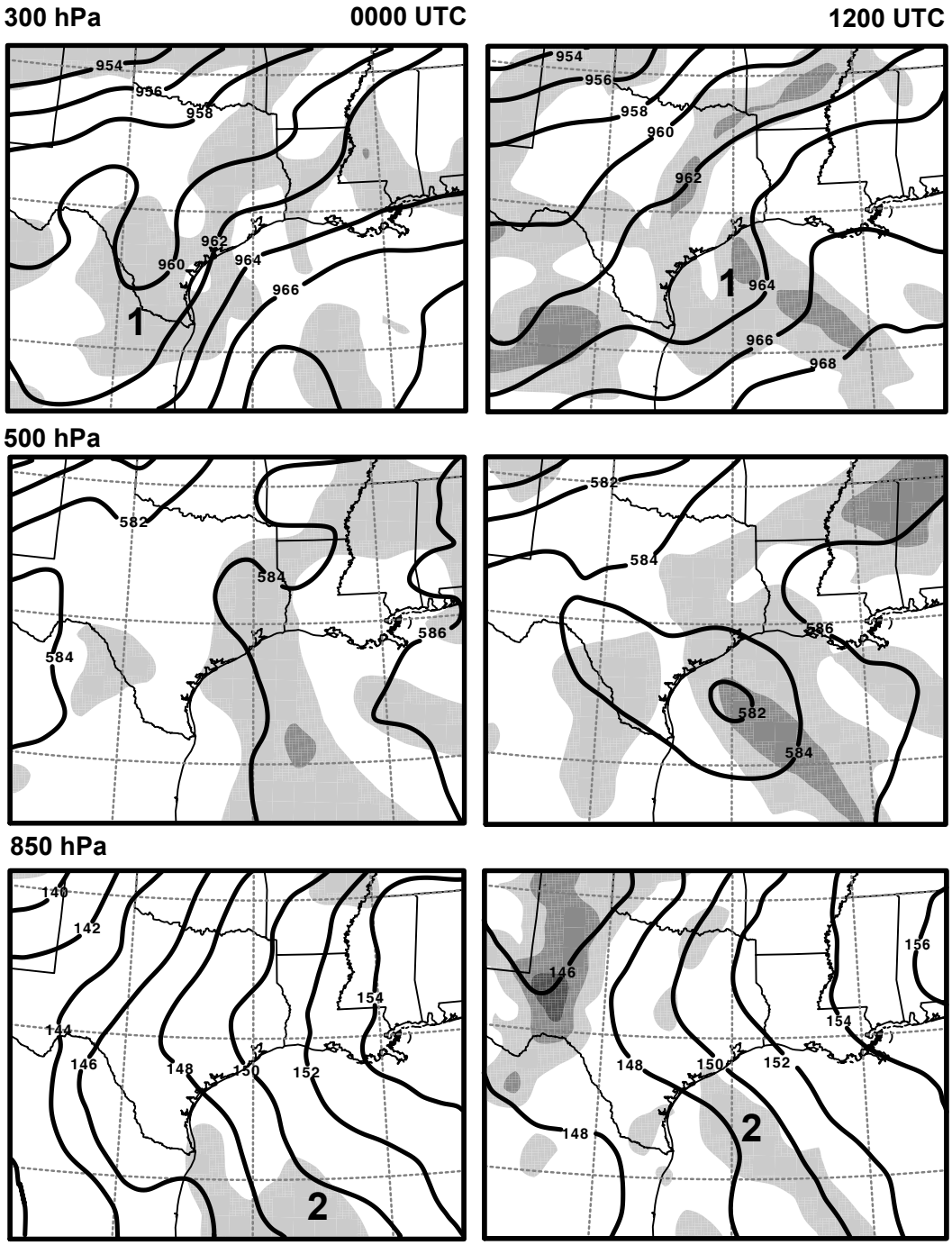

FIG. 6: 0000 UTC and 1200 UTC 5 June ETA analysis of average potential vorticity in 100 hPa layers and height fields. Layers are centered at 300 hPa, 500 hPa, and 850 hPa. Shading is in 0.5 PV Unit (1 PVU = 1.0 x 10^6 m^2 K kg^{-1} s^{-1}) increments, starting at 0.5 PVU. Bold 1 used to indicate upper-level trough and bold 2 used to indicate low-level PV anomaly mentioned in text.

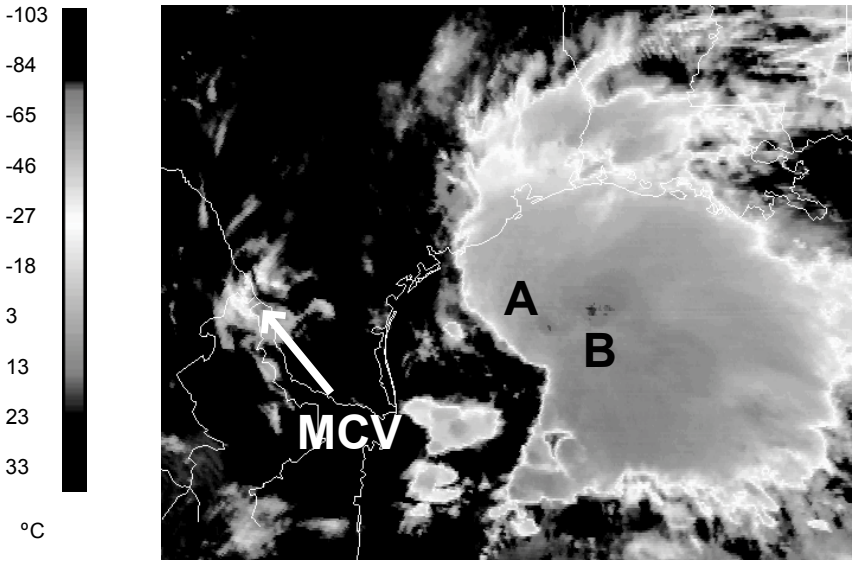

FIG. 7: GOES 8 IR image of Allison at 1145 UTC 5 June. The colder cloud-top temperatures are coincident with the stronger reflectivity values in Fig. 8. The cold cloud tops near A and B are coincident with the primary and secondary circulation centers and the white arrow denotes the general area of a remnant MCV over Mexico.

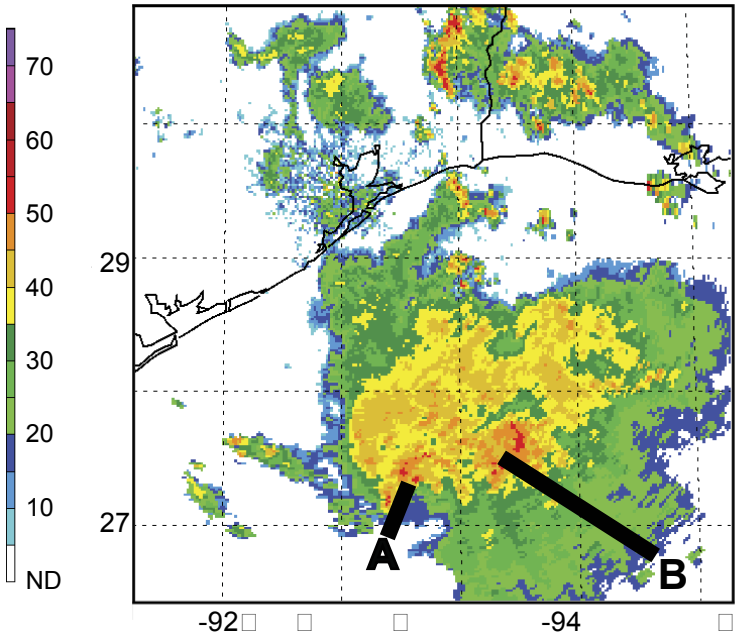

FIG. 8: KHGX Doppler radar image from 1202 UTC 5 June. As in Fig. 7, the locations of circulation centers A and B are indicated. Scale on left is in dBz. NIDS format radar data is utilized for this study.

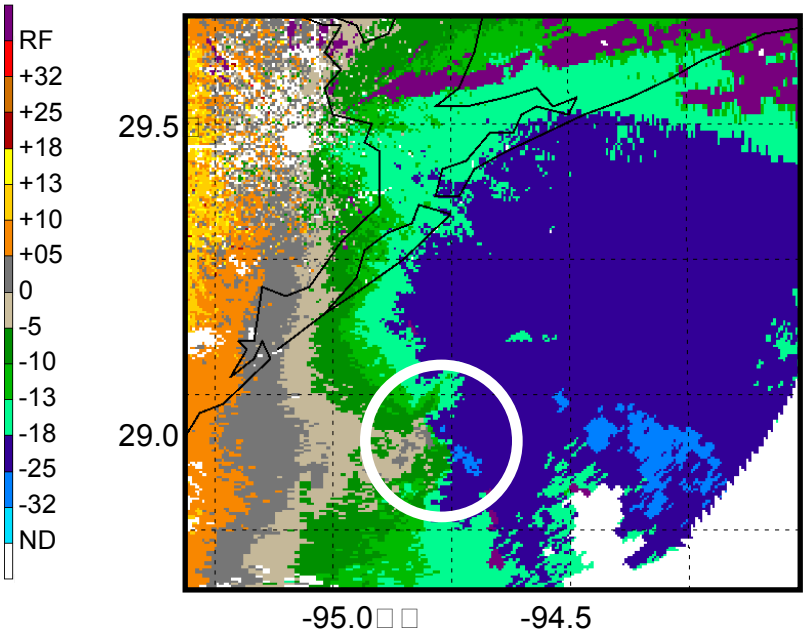

FIG. 9: League City base velocity at 1913 UTC 5 June. Scale on left is in m s^{-1}. Approximate center of vortex A is located at the center of the white circle. The circle radius is approximately twice the RMW of A.

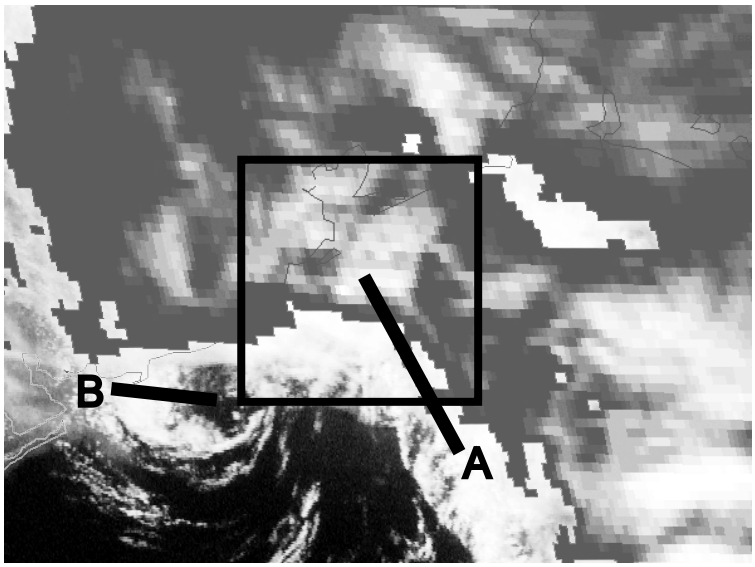

FIG. 10: Overlay of GOES 8 IR and visible images from 1915 UTC 5 June. IR overlay starts at temperatures of -30ºC and enhancement starts at cloud top temperatures of about -50ºC. The coldest cloud tops in this image are about -65ºC. Black box denotes area covered in Fig. 9. The approximate centers of vortices A and B are noted.

b. Meso-β-scale vortices

While synoptic- and meso-α- scale PV superposition evidently aided in Allison's initial formation, meso-β-scale PV interaction became important hours later. Radar and satellite image loops give convincing evidence for two meso-β-scale vortices within this storm. For the purpose of this study, they will be referred to as "A" and "B."

Fig. 8 shows the distinct reflectivity maxima associated with the centers of the vortices, while the velocity and visible satellite imagery in Figs. 9 and 10 show evidence of circulations with each center. The meso-β-scale circulation associated with A is evident in the velocity data in Fig. 9, but B did not show up well in radar data at this time because it was convectively inactive. However, Fig. 10 shows a distinct low-level cloud swirl that is obviously associated with a circulation (vortex B) when viewed in a visible satellite loop. The individual centers are difficult to detect from the mesoscale analyses in Fig. 4 because these analyses are drawn to depict the storm-scale features. Other surface observations not included confirm that these meso-β-scale vortices extended to the surface.

In order to determine where these vortices originated, how they interacted with one another and with their surroundings, and how long each survived, they were both tracked from their point of origin until after the storm made landfall (Fig. 11a). Radar reflectivity loops indicate that a vortex, possibly the aforementioned MCV, likely existed at the time of convective initiation near where A was first tracked. In addition to using reflectivity data to track the circulation center of A, Doppler velocity data is used when possible to verify track in Fig. 11a.

Range-folded velocity data and lack of an obvious circulation in reflectivity data prevents direct tracking of B until that center is out of the range-folded region at about 1530 UTC. At this time, B is coincident with a distinct convective maximum that formed near 1030 UTC about 160 km to the east of A. The track for B in Fig. 11 assumes that a circulation existed soon after initiation of the aforementioned convective maximum and follows the center of that feature until 1530 UTC. From this point, a similar method of tracking A is used, but with the aid of visible satellite imagery when its convection dissipated.

In order to investigate the mesoscale kinematic structure of Allison, high-density (30 second) flight-level reconnaissance observations were supplemented with KHGX velocity data to derive the analysis shown in Fig. 12. The KGHX velocity data proved useful for analyzing vortex A because it was poorly sampled by reconnaissance aircraft. On the other hand, abundant reconnaissance observations within B compensate for poor sampling of the vortex by the KGHX radar. The nominal time of this analysis is about 1915 UTC and it approximates the wind field at 250 m. The observations shown were taken from about 1810 UTC until 1940 UTC. Vortex B was nearly stationary during this time (see Fig. 11a), so this analysis is approximately equivalent to a reference frame moving with the center of B. Vortex A was moving northeastward at about 8 m s^{-1} during this period.

Figure 12 reveals a complex mesoscale wind pattern associated with Allison. Two wind-shift lines shown in Fig. 12 terminate at or near the center of vortex A. One extends southwestward through B, and the other extends southeastward. The wind direction

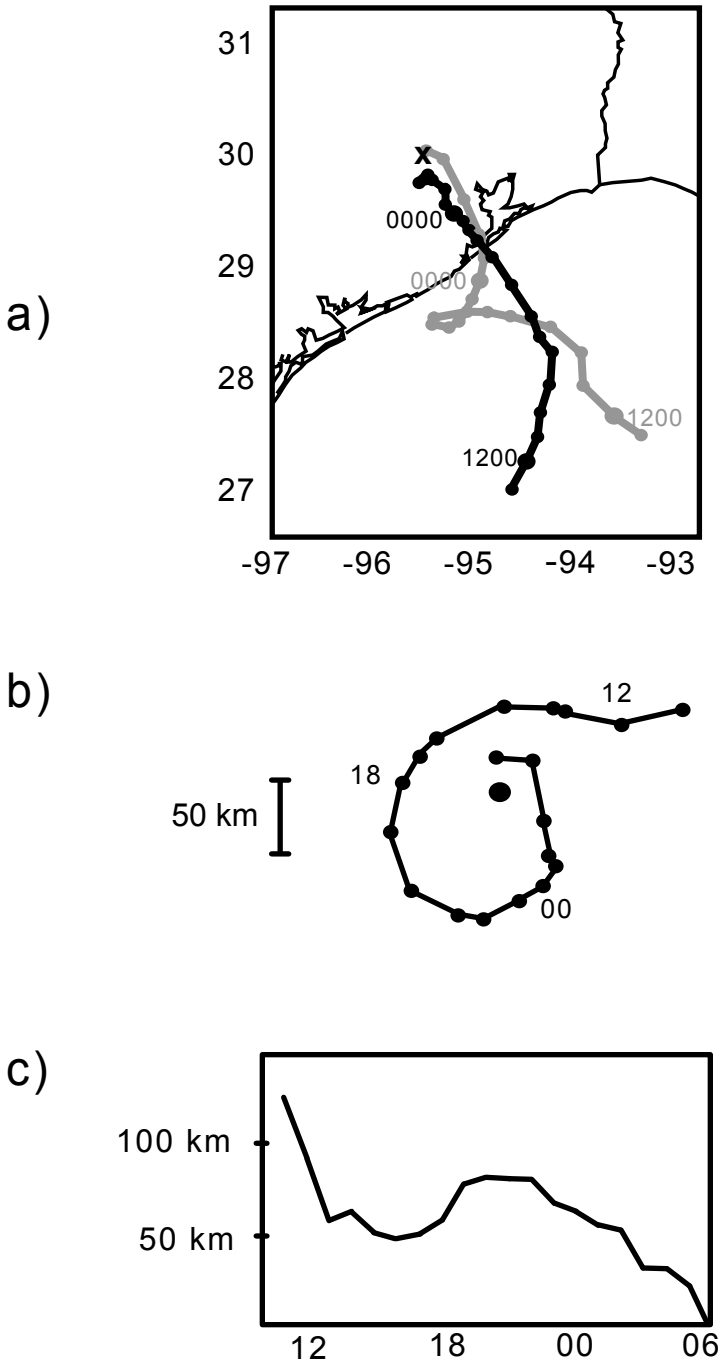

FIG. 11: An analysis of A and B via: a) radar and satellite estimated tracks the vortices; b) position of B relative to A; and c) distance between the two vortices. In a, the track of vortex A is shown in black, and that of B is in gray. The individual points mark the location of each vortex in one hour time steps, and the positions at 1200 UTC 5 June and 0000 UTC 6 June are marked for reference. The black X at the end of the paths marks the spot at which the two vortices became indistinguishable from one another (between 0500 UTC and 0600 UTC).

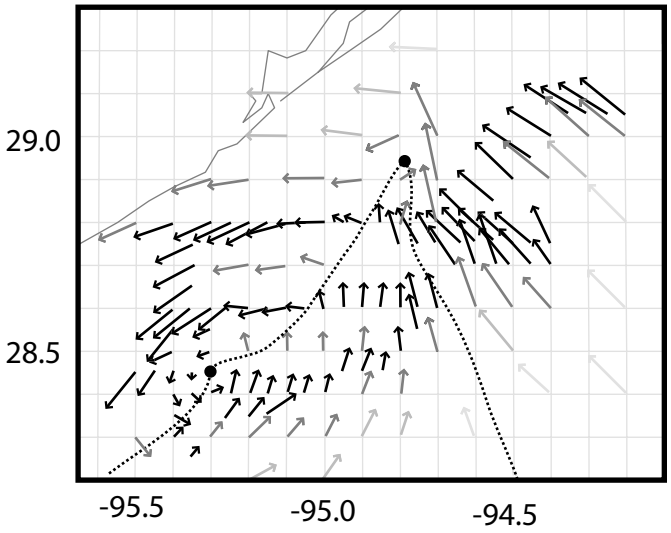

FIG. 12: Flight level (~250 m) wind analysis. The data utilized are high resolution reconnaissance observations and KHGX radial velocity, and the nominal time is 1915 UTC on 5 June. Arrows are shaded according to certainty, with higher confidence represented by darker shades. The dashed lines represent the positions of wind shifts.

shifted about 60º over 5 km along the westernmost line. While the change in wind across the easternmost line for the area analyzed in Fig. 12 was mostly in strength, the wind shifted by about 60º over 20 km further south along the line. The winds south and west of the two wind-shift lines (generally between the two vortices) were much weaker than those north and east of the wind shifts.

Although the two vortices appeared to be about the same size, their kinematic properties differed significantly at the time of the analysis. Available data indicate that the radius (defined for all vortices herein as the radius at which the flow induced by the vortex becomes indiscernible from variations in the background wind field) of each vortex was

about 20 km. No deep convection was occurring within this distance from the center of B at the analysis time, and the weak winds near the center *increased* to the magnitude of the background winds near the radius of the vortex. Meanwhile, the strongest winds observed with the convectively active vortex A were within a few kilometers of the center. From a point of reference following the center of A, the wind strength *decreased* to the strength of the background winds at the vortex radius.

The cyclonic movement of each center relative to the other was likely due to advection by winds associated with the larger-scale PV anomalies rather than due to interaction between the small-scale vortices. While the radius of each vortex was about 20 km, the distance between the two vortices shown in Fig. 11 was greater than 50 km until 0300 UTC 6 June. Meanwhile, the observed rate of rotation of B relative to A was at least $8 – 10$ m s^{-1}. Mutual interaction cannot explain that rate of rotation at such a large distance relative to the estimated radii.

Vortices A and B merged on the northwest side of Houston and produced a larger single vortex with a greater pressure perturbation. The mesoscale surface analyses in Fig. 4 reveal the evolution to a more concentrated vortex with stronger pressure gradients. The lowest surface pressure measured as Allison made landfall was no less than 1004 hPa, but the central pressure fell to less than 1003 hPa north of Houston even as deep convection weakened. Note that the central pressure fell in spite of the environmental tendency for pressure rises and resulted in the stronger pressure gradients in Fig. 4c. Although one criterion for system strengthening was met when the surface pressure dropped, the surface winds did not respond. This is partly due to the increased surface friction over land and

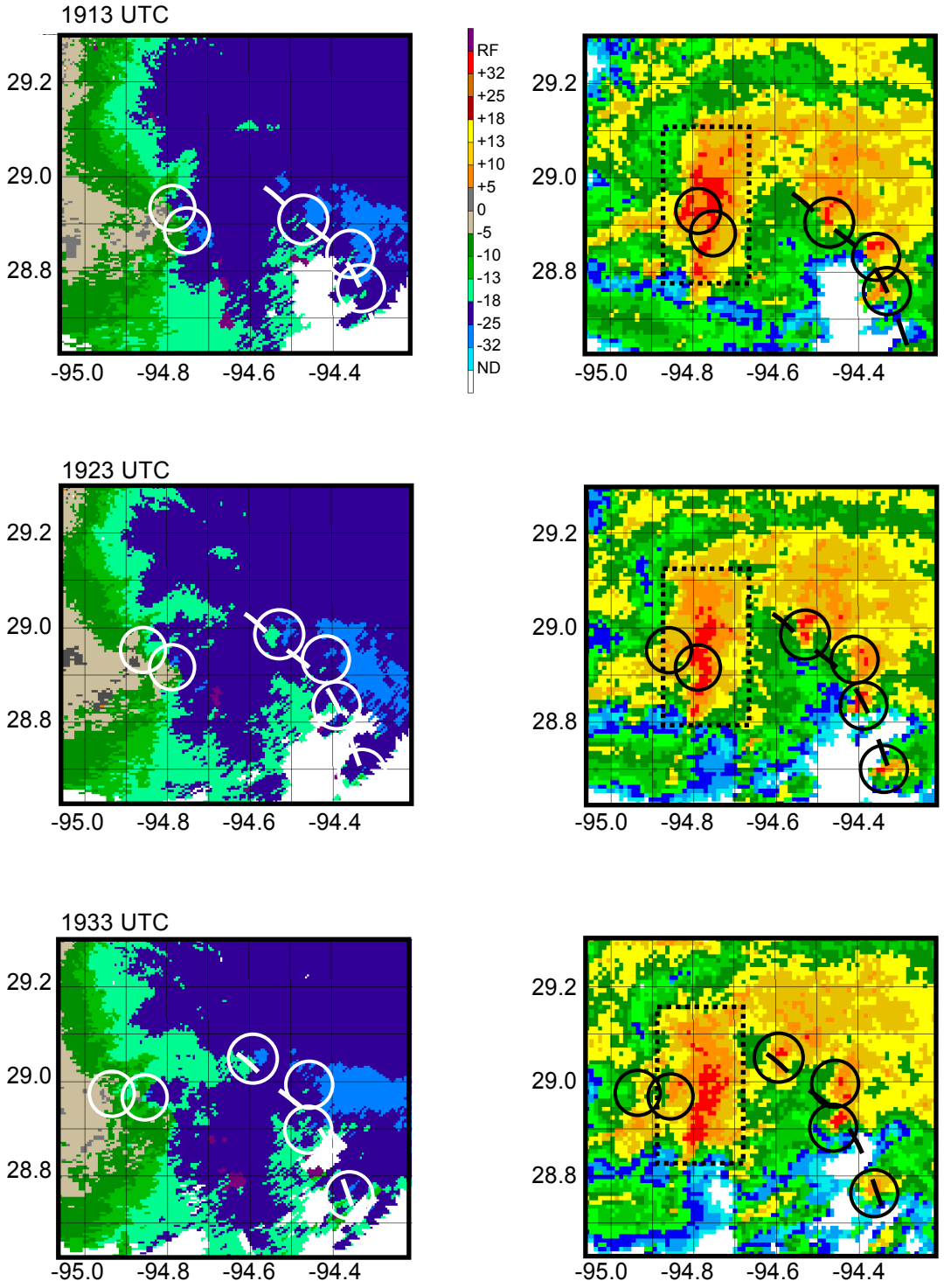

FIG. 13: League City Doppler velocity and reflectivity images from 5 June. For reference, meso-γ-scale vortices discussed in text are located at center of circles. Circle radius is approximately twice the associated vortex radius of maximum winds. Velocity scale is in m s^{-1}, and reflectivity scale is same as in Fig. 8. Shear/rainband axis is denoted by white (black) dashed line in velocity (reflectivity) data. Convection enclosed by dotted line is referred to as "central core convection."

the ongoing dissipation of deep convection near the merged centers. However, had this merger taken place over water, intensification might have resulted.

c. Meso-γ-scale vortices

It became apparent as vortex A neared the KHGX radar that meso-γ-scale vortices associated with single convective cells were embedded within the meso-β-scale vortex. These vortices, shown in Fig. 13, existed both in the core of convection near the center and in the primary rainband (for reference, these areas are labeled in Fig. 13). The typical radius of these vortices was less than 5 km while that of their parent convective cells that was less than 2.5 km. The vorticity within these features was estimated from the NIDS-format velocity data by approximating the maximum inbound and outbound velocities at the radius of maximum wind (RMW) of each vortex. For most of these features the vorticity ranged from about 10^{-3} s^{-1} to 10^{-2} s^{-1}, and it peaked near 1.5×10^{-2} s^{-1} in the strongest vortex for only a short period of time. The vortices tended to be fairly shallow, with the strongest vorticity generally measured in the lowest radar elevations at about 1 km above ground level. With one exception discussed below, the highest low-level reflectivity associated with these convective cells was very near or over the low-level vortex center.

While the Doppler-indicated rotational velocities of the strongest vortices tended to be only as strong as moderate Great Plains mesocyclones (reference 6.5 km nomogram developed by the WSR-88D Operational Support Facility), their characteristic velocities and scales were comparable to tornadic mesocyclones observed with other Gulf of Mexico tropical systems documented by Spratt et al. (1997). The rotational velocities of these

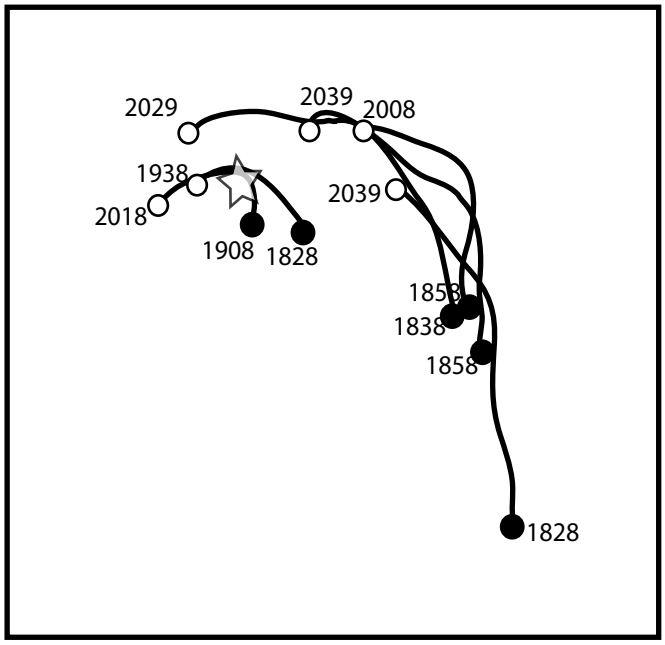

FIG. 14: Tracks of all meso-γ-scale vortices relative to meso-β-scale center A (represented by star) that formed between 1830 and 1930 UTC 5 June. Tracks of A' and vortices associated with A' itself are not plotted. Filled circles represent points at which the convective cell associated with each vortex attained precipitation intensity of 50 dBZ. Hollow circles indicate point at which vortex was no longer trackable.

mesocyclones and those observed with Allison generally ranged from 7.5 m s^{-1} to 15 m s^{-1} . The typical RMW with Allison's meso-γ-scale vortices averaged between 1.5 km and 2 km, while those investigated by Spratt et al. (1997) ranged from 1 km to 1.5 km. Finally, the radius of Allison's meso-γ-scale vortices generally extended to about 5 km.

The tracks of all such vortices that formed between 1830 UTC and 1930 UTC are plotted in Fig. 14 relative to vortex A. Although such features likely existed before this time, the distance of the system from the radar and shallow vortex depth inhibited their

detection at earlier times. Also, the vortices that formed after 1930 UTC associated with center A' (discussed below) are not plotted in Fig. 14 to eliminate confusion. Every plotted vortex formed to the southeast of and moved cyclonically around meso-β-scale center A. These vortices tended to have two distinct fates; they either dissipated to the northwest of A or they became ingested into the deep convection east and north of its center.

It is important to note the environment of the area where these vortices formed. As previously discussed, the superposition of Allison onto a background pressure gradient yielded higher surface winds on the east side of the storm. This concept also applies to the wind field around vortex A. The aforementioned convective cells were likely fed by the resultant higher surface fluxes immediately east of A. They then dissipated on the west side of the vortex where weaker surface winds likely resulted in reduced surface fluxes. In addition, the mesocyclones formed within the RMW of vortex A or along a shear axis associated with the primary rainband (see Fig. 13). These were both areas of locally enhanced cyclonic vorticity, which likely aided in mesocyclone development.

The most interesting meso-γ-scale vortex observed formed near the southern extent of the central core convection shortly before 2000 UTC. While this vortex (hereafter referred to as A') initially had characteristics similar to the other meso-γ-scale vortices, its evolution (shown in Fig. 15) had a profound impact on the structure of the storm. At 2018 UTC A' had an RMW of approximately 1 km and a vortex radius of less than 2.5 km. However, within three hours its RMW and vortex radius had expanded respectively to about 5 km and to between 10 and 15 km. The rotational velocity (one half the sum of the maximum inbound and outbound velocities) of this vortex increased with

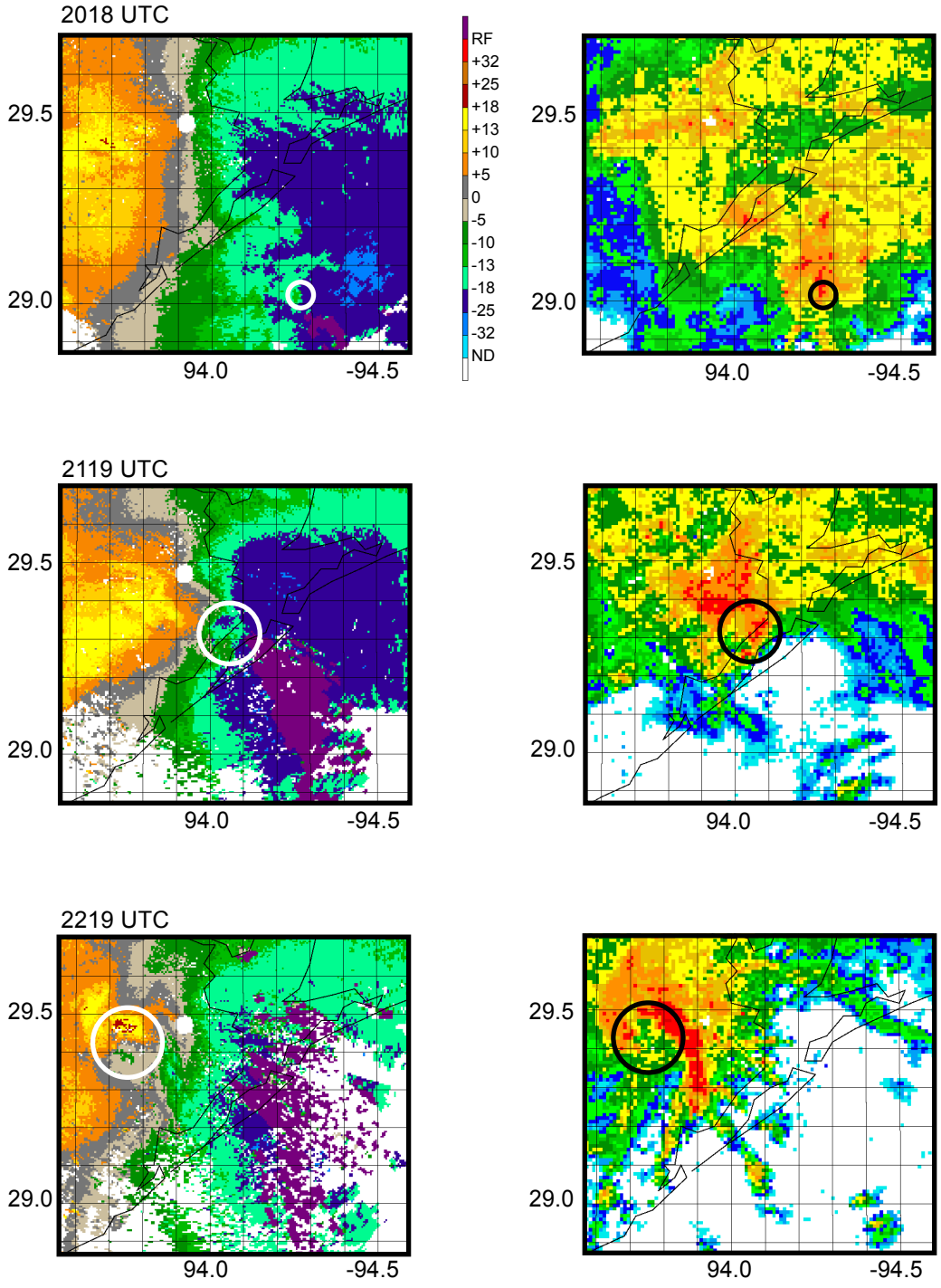

FIG. 15: The growth and development of A' as seen in League City Doppler velocity and reflectivity images from 5 June. Vortex is located at center of circles and circle radius is approximately twice the associated vortex RMW. Velocity scale is in m s^{-1}, and reflectivity scale is same as in Fig. 8.

the RMW such that the estimated value of vorticity (approximately 5×10^{-3} s^{-1}) within the RMW did not change. Also, the dramatic upscale growth of A' made it of comparable size to meso-β vortex A. A' quickly became the strongest meso-β-scale vortex within Allison. After about 2000 UTC, the center of A became increasingly difficult to follow using Doppler velocity data. For the next several hours, only a diffuse area of weak cyclonic vorticity with A could be inferred from the velocity data. Reflectivity data also showed little evidence of a circulation. Meanwhile, by 2200 UTC, both the vortex radius and the RMW of A' had expanded into the meso-β scale. With nearly all the deep convection rotating exclusively about A', it had become the most visible meso-β-scale vortex in radar data.

The convective structure of A' exhibited dramatic changes as the vortex grew. During the early stages of vortex growth, the size of its >50 dBZ isopleth expanded dramatically. While it had been 1 – 2 km wide at 2018 UTC, it steadily grew to 7 – 8 km across by 2149 UTC. Up until this point, the highest reflectivity remained nearly superposed upon the vortex, much like with the previously observed vortices of the same scale. Figure 15 shows how this changed within the next 30 minutes as the vortex continued its upscale growth. The deep convection over the center of A' substantially weakened as a large band of 45 – 60 dBZ convection developed and encircled more than 50% of the vortex near its RMW.

This evolution is markedly similar to that observed during the formation of the eye of Tropical Cyclone Ed early during its genesis phase (Stewart and Lyons 1996). The authors of that study hypothesized that a rapid increase in the low-level wind field about a

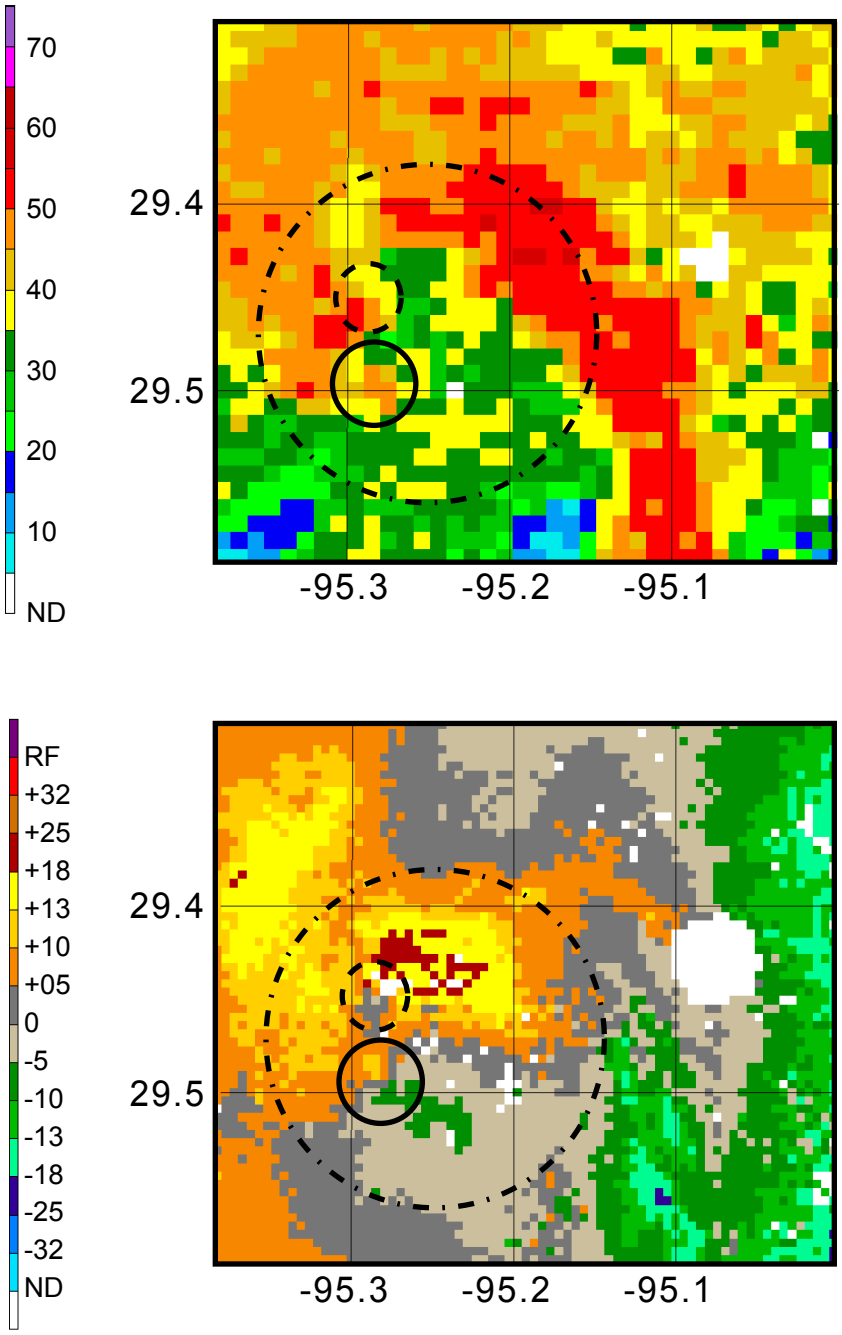

FIG. 16: Vortex A' and associated meso-γ vortices at 2219 UTC 5 June. Meso-γ-scale vortex discussed in paper is at center of solid circle, and another possible vortex is at center of dashed circle. Center of vortex A' is at center of dot-dash circle. Radius of circles is approximately twice that of RMW of the encircled vortex. Reflectivity scale is in dBZ and wind scale is in m s^{-1} .

small meso-β-scale vortex was the result of a large convective burst within the tropical depression. They further hypothesized that this wind field quickly became supergradient and induced subsidence within the RMW. In support of this hypothesis, the convection near the vortex center quickly died while a band of precipitation encircled the vortex near the RMW, forming the eye of what would eventually become Ed. Although this nascent eyewall was only composed of 25 – 35 dBZ convection, Stewart and Lyons (1996) report that this vortex remained the eye even as Ed strengthened to supertyphoon strength.

Figure 16 shows that at least one meso-γ-scale vortex formed within the wall of deep convection surrounding the center of A' during the hour when it was most organized. This vortex, while smaller than any other tracked in this study, was the most intense vortex observed. With an RMW at times of only 1 km (putting it at borderline microscale) and a rotational velocity around 17 m s^{-1}, the resultant vorticity was over 1.75×10^{-2} s^{-1}. Like the other meso-γ-scale vortices of the day, this vortex tended to be associated with a local maximum in reflectivity and rotated counterclockwise around the local meso-β vortex. It formed on the northeast side of A', attained its maximum strength on the west side of vortex, and dissipated on the southwest side. The vortex evolution was rapid; the time between formation and dissipation was between 20 and 25 minutes. There were other possible meso-γ-scale vortices of similar size and strength within the wall of deep convection. However, these features lasted only one to two volume scans, rendering them difficult to track.

As A' continued to move inland, it rapidly became more disorganized. By 2300 UTC A' had become somewhat separated from the deep convection as it moved farther

west. While the vorticity had not substantially decreased, the vortex was now only surrounded about 30% by 30 dBz convection. After 2300 UTC, the vortex itself began to rapidly weaken, and by shortly after 0100 UTC, any semblance of a circulation in the reflectivity or velocity data had completely vanished.

4. DISCUSSION

a. Other cases and forecasting issues

The occurrence of multiple meso-β-scale vortices presents a difficulty in tracking developing tropical cyclones. In the 2003 season alone, the presence of such features complicated TPC tracking of at least four Gulf of Mexico tropical systems (Bill, Claudette, Henri, and Grace). One particular discussion for Claudette indicated that the feature being tracked as the center appeared to be rotating around a broader circulation. Furthermore, TPC discussions often speak of the center of circulation jumping from one convective flare-up to another, with multiple candidates for the true circulation center. This often happens in high-shear cases when convection gets displaced downshear of a circulation center, resulting in pressure falls and center reformation under the convection. The fates of these circulation centers vary; while some merge (as with A and B in Allison), some eventually dissipate in the absence of sustaining convection (as with A' in Allison).

While difficulty in pinpointing the exact center of developing tropical cyclones is of little consequence over the open ocean, it becomes a concern when such systems near land. Tracking a single vortex as the center can mean the landfall of another vortex and its associated weather hundreds of kilometers from where the official center is being tracked. In the case of Allison, convection-free vortex B was tracked as the official center as A, A', and the associated convection moved over the suburbs of Houston. Similar events happened with tropical storms Fay (2002) and Grace (2003), which made landfall near the upper Texas coast. As was the case with Allison, tropical storm force

winds and major flooding often accompany these other, well-defined centers while mostly clear skies and light winds might accompany the official center.

b. Hot towers and vortical hot towers

The meso-β-scale convective vortices in Allison had several properties in common with the "vortical hot towers" (VHTs) simulated and discussed by Hendricks et al. (2004) and Montgomery et al. (2004, submitted for publication to *J. Atmos. Sci.*). The typical VHT simulated by Hendricks et al. (2004) with a 3-km grid spacing had approximately a 10 km wide updraft and had a RMW of about 7.5 km. The approximately 6.5 km RMW and 12.5 m s^{-1} rotational velocity associated with A also compared favorably with these simulated features.

Despite this, other important differences make it unclear how the meso-β-scale vortices actually relate to the simulated VHTs. The structure and scale (15 – 30 km) of the reflectivity pattern associated with A imply a complex of individual updrafts. These updrafts stimulated significant asymmetries in the circulation of A on a scale that the aforementioned numerical simulations could not have resolved. Under the assumption that the smallest resolvable features in a numerical simulation are five times the grid spacing, the 15 km wide VHTs in these numerical studies were the smallest structures that could be resolved by Hendricks et al. (2004). The VHTs in that study were consequently limited to axisymmetry. Their investigation also noted that finer-resolution numerical simulations tended to produce smaller VHTs than with the 2 km or 3 km studies. Thus, it is uncertain if the features simulated are an attempt by the model to produce meso-γ-scale vortices or if they are poorly-resolved meso-β-scale vortices.

Regardless of how these vortices relate to VHTs, the fact that meso-γ-scale vortices existed within the meso-β-scale vortices is important. While the meso-β-scale vortex merger is likely significant for tropical cyclone scale intensification, the above observations suggest that smaller vortices and individual updrafts are the actual building blocks of and source of PV production for the meso-β-scale vortices. To our knowledge, this phenomenon has yet to be observed in any published numerical study because the scale is too small. Any grid spacing larger than 0.25 – 0.5 km is inadequate to resolve meso-γ-scale vortices which have an RMW of approximately 2 km. Computing power is only now advancing to the point where such three-dimensional simulations are possible on the scale of a tropical system.

While the relationship between vortices A and B and the simulated VHTs remain ambiguous, the observed meso-β scale features are not the same as the hot towers discussed in previous studies. Although the intrinsic scale of a hot tower does not seem to have been formally defined in peer-reviewed literature, the term has historically referred to individual cumulonimbi with approximately 5 km wide updrafts (e.g. Reihl and Malkus 1958, Malkus et al. 1961, and Simpson et al. 1998). As indicated above, the structure and scale of the deep convection associated with A imply a complex of individual updrafts rather than a single hot tower. Instead, the hot towers of Allison were likely the convective cells associated with the meso-γ-scale vortices.

c. Commonality of meso-β- and meso-γ- scale vortices

It is difficult to say to what extent multiple meso-β- and meso-γ- scale vortices are a normal stage of tropical cyclone development. Multiple meso-β-scale vortices

have only been documented by Stossmeister and Barnes (1992), Hendricks et al. (2004), and the present study. Furthermore, the importance of multiple meso-γ-scale vortices in a developing tropical cyclone has only been discussed by Stewart and Lyons (1996). Despite the relative absence of observations of these smaller-scale vortices in studies relevant to tropical cyclone formation, the supercell characteristics of rainband and eyewall meso-γ-scale vortices of mature tropical cyclones have been extensively documented in the literature (e.g., Spratt et al. 1997). Furthermore, the frequent appearance meso-β-scale vortices in TPC forecast discussions indicates that they are fairly common.

The small scales of these vortices make them exceptionally difficult to observe in many cases. Meso-β-scale vortices can be only be remotely detected by Doppler radar or in visible satellite imagery if their convection dissipates and the low-level cloud swirl becomes exposed. It is for this reason that sheared environments result in the most easily observable meso-β-scale vortices when storms are far from shore. Even with insitu airplane observations, these vortices can be missed (e.g., as shown in Fig. 12, aircraft reconnaissance never directly observed vortex A). Meanwhile, meso-γ-scale vortices can only be observed with Doppler radar. Their scale is much too small to be directly observed even with airplane data.

5. CONCLUSION

An investigation of a developing tropical cyclone has been presented with emphasis on the interaction and superposition of PV anomalies on multiple scales. It is clear in this case that PV superposition is likely a key component of cyclogenesis from the lower synoptic to the lower meso-γ scales. While only the case of Allison has been discussed in great detail, other studies have documented PV superposition on various scales. In addition, the clear presence of multiple mesoscale vortices in many developing tropical cyclones indicates that such superposition *could* be important for most tropical cyclones.

While mesoscale vortices are of great interest for understanding tropical cyclogenesis, they also present considerable forecasting implications. A significant forecasting problem lies in the paradigm that, given a tropical cyclone, an exact center of circulation must exist. Although this idea works well for well-developed systems, such as a hurricane with an eye, it is inappropriate for a developing tropical storm. Rather, the tendency is for developing systems to be composed of a diffuse area of elevated PV with small, concentrated areas of particularly high PV. The transient nature of the small areas of high PV renders them poor predictors of long-lived centers. With this perspective, it seems logical that the practice of determining an exact center should be abandoned until an eye emerges with a particular system.

Although it is clear from the previous discussion that an exact center does not exist for many developing tropical cyclones, a method for providing an estimated system center is still necessary if an agency wishes to track and name such systems. Given the

continued public and TPC interest in the tracking and naming of tropical depressions and storms, several alternatives to the current tracking method are outlined in Table 1. The advantages and drawbacks are listed in this table for each potential method of tracking. Note that vortices of interest in this table are on the meso-β scale, the smallest observable scale with reconnaissance observations.

The most desirable methods should have the advantages of providing a *complete* picture, being *flexible* for many users, and estimating a center *central* to all vortices. A complete picture consists of position and strength information on all meso-β and larger scale vortices within a particular system. Less complete methods ignore part or all of the meso-β-scale storm structure. *Flexible* methods contain information that can be filtered according to the needs of different users. For example, a broadcast meteorologist in a particular coastal city might only need specific information on a vortex approaching that city while a research scientist might need information on *all* vortices at a given time. In any event, a center that is central to all given vortices is easily estimated once one has the needed information on all meso-β and larger scale vortices at a particular time. A central center estimate is important because it deemphasizes single vortices and forces the forecaster and the public to focus on the system as a whole.

There are also drawbacks to any method of tracking a tropical cyclone. The more complete methods tend to require more *reconnaissance*, which can be costly and is impossible for storms out of reach of reconnaissance aircraft. In addition to being more costly, these methods are also more *complex* because of the necessary increase in data that has to be communicated. Finally, the less complete methods have the drawback of

TABLE 1. Potential tracking methods with advantages and drawbacks for each.

Method	Advantages				Drawbacks			Score
	Complete	Flexible	Central		Recon	Complex	Continuity	
Strength-weighted average vortex position	+ + + + + Provides most complete picture	+ + + + + Filter data according to user needs	+ + + + + Center central to all vortices		- - - - - Most recon-naissance time	- - - - - Most data to interpret		5
Average vortex position	+ + + + Provides nearly complete picture	+ + + + + Filter data according to user needs	+ + + + + Center central to all vortices		- - - - Signif-icant recon-naissance time	- - - - Much data to interpret	- - Discontin-uous track possible with transient vortices	4
Geometric center of smallest closed isobar	+ + Gives some attention to individual vortices		+ + + + Center likely to be central to vortices		- - Requires recon-naissance time to find isobar	One simple point	- - - - Multiple closed isobars and isobar obliquity possible	0
Geometric center of largest closed isobar	Ignores internal vortices		+ Non-central location possible		Larger-scale isobar easier to estimate	One simple point	- - - Multiple closed isobars may exist	-2
Strongest vortex + radius to furthest vortex	+ + + Correctly conveys tracking uncer-tainty		Non-central location likely		- - - Recon-naissance time to find strongest vortex	-	- - - - Discontin-uous track likely as centers form and decay	-5
Most easily identified vortex	Conveys little inform-ation		Non-central location likely			One simple point	- - - - - Discontin-uous track likely	-5

producing a discontinuous estimated storm track. This center repositioning is commonly seen with the current method of tracking tropical cyclones.

While all approaches to tracking have their strengths and weaknesses, it appears that advantages strongly outweigh drawbacks for the more complex methods. The system currently employed to track developing tropical cyclones is comparable to the least complex method listed while the more desirable alternatives more completely convey important information. Data on meso-β-scale vortex positions is clearly advantageous for landfalling systems and would mitigate public scrutiny and forecaster disagreement on center position. Another appealing advantage is the ability to convey a subset of complex information to less sophisticated users.

Although Tropical Storm Allison provides an interesting glimpse into rarely documented mesoscale processes in tropical cyclogenesis, many of the observations and conclusions drawn herein are subject to the limitation of coming from a single case. For example, the commonality or importance of the documented meso-γ-scale vortices to tropical cyclogenesis in general remains unknown. Few published observational studies have focused on meso-β or meso-γ scales. Although this is at least partly due to a lack of data over the ocean, the occurrence of landfalling tropical cyclones in their development stage is common enough that other similar studies are possible. Detailed analyses of other cases should address much of this uncertainty and provide for a more complete understanding of tropical cyclone formation.

REFERENCES

Craig, G. C., and S. L. Gray, 1996: CISK or WISHE as the mechanism for tropical cyclone intensification. *J. Atmos. Sci.*, **53**, 3528-3540.

Davis, C., and L. F. Bosart, 2001: Numerical simulations of the genesis of Hurricane Diana (1984). Part I: Control simulation. *Mon. Wea. Rev.*, **129**, 1859-1881.

DeMaria, M., Knaff, J. A., and B. H. Connell, 2001: A tropical cyclone genesis parameter for the tropical Atlantic. *Wea. Forecasting*, **16**, 219–233.

____, and J. M. Gross, 2003: Evolution of prediction models. *Hurricane! Coping with Disaster: Progress and challenges since Galveston, 1900*, R. Simpson, Ed., American Geophysical Union, 103-126.

Emanuel, K. A., 1986: An air-sea interaction theory for tropical cyclones. Part I: Steady-state maintenance. *J. Atmos. Sci.*, **43**, 585-604.

____, 1989: The finite-amplitude nature of tropical cyclogenesis. *J. Atmos. Sci.*, **46**, 3431-3456.

____, 2003: A century of scientific progress: An evaluation. *Hurricane! Coping with Disaster: Progress and challenges since Galveston, 1900*, R. Simpson, Ed., American Geophysical Union, 177-204.

Gray, W. M., 1968: Global view of the origin of tropical disturbances and storms. *Mon. Wea. Rev.*, **96**, 669-700.

Harr, P. A., Elsberry, R. L., and J. C. Chan, 1996: Transformation of a large monsoon depression to a tropical storm during TCM-93. *Mon. Wea. Rev.*, **124**, 2625-2643.

Hendricks, E. A., Montgomery, M. T., and C. A. Davis 2004: The role of "vortical" hot towers in the formation of tropical cyclone Diana (1984). *J. Atmos. Sci.*, **61**, 1209–1232.

Hoskins, B. J., M. E. McIntyre, and A. W. Robertson, 1985: On the use and significance of isentropic potential vorticity maps. *Q. J. R. Meterol. Soc.*, **111**, 877-946.

Malkus, J. S., C. Ronne, and M. Chaffee, 1961: Cloud patterns in Hurricane Daisy. *Tellus*, **13**, 8-30.

McBride, J. L., and R. Zehr, 1981: Observational analysis of tropical cyclone formation. Part II: Comparison of non-developing versus developing systems. *Jour. Atmos. Sci.*, **38**, 1132-1151.

Raymond, D. J., and H. Jiang, 1990: A theory for long-lived mesoscale convective systems. *J. Atmos. Sci.*, **47**, 3067-3077.

Reihl, H., and J. S. Malkus, 1958: On the heat balance in the equatorial trough zone. *Geophysica*, **6**, 503-538.

Ritchie, E. A., and G. J. Holland, 1997: Scale interactions during the formation of Typhoon Irving. *Mon. Wea. Rev.*, **125**, 1377-1396.

Rotunno, R., and K. A. Emanuel, 1987: An air–sea interaction theory for tropical cyclones. Part II: Evolutionary study using a nonhydrostatic axisymmetric numerical model. *J. Atmos. Sci.*, **44**, 542-561.

Simpson, J., E. Ritchie, G. J. Holland, J. Halverson, and S. Stewart, 1997: Mesoscale interactions in tropical cyclone genesis. *Mon. Wea. Rev.*, **125**, 2643-2661.

____, J. B. Halverson, B. S. Ferrier, W. A. Peterson, R. H. Simpson, R. Blakeslee, and S. L. Durden, 1998: On the role of "hot towers" in tropical cyclone formation. *Meteorol. Atmos. Phys.*, **67**, 15-35.

Spratt, S. M., Sharp, D. W., Welsh, P., Sandrik, A., Alsheimer, F., and C. Paxton, 1997: A WSR-88D assessment of tropical cyclone outer rainband tornadoes. *Wea. Forecasting*, **12**, 479–501.

Stewart, S. R., and S. W. Lyons, 1996: A WSR-88D radar view of tropical cyclone Ed. *Wea. Forecasting*, **11**, 115–132.

Stossmeister, G. J., and G. M. Barnes, 1992: The development of a second circulation center within Tropical Storm Isabel (1985). *Mon. Wea. Rev.*, **120**, 685–697.

VITA

Jason Allen Sippel

ADDRESS:
Department of Atmospheric Sciences
Texas A&M University
3150 TAMU
College Station, TX 77843-3150

EDUCATION:

B.S. Meteorology, Texas A&M University
Graduated May 2002

M.S. Atmospheric Sciences, Texas A&M University
Graduated December 2004

PUBLICATIONS:

Sippel, J., 2001: Numerical Simulation of the Genesis of Tropical Storm Allison (2001). Preprints, *19th Conf. on Numerical Weather Prediction*, San Antonio, TX, Amer. Meteor. Soc., 361-364.